Seasonal prediction of springtime tornado activity in the United States using a hybrid model

Authors: Matthew Graber[1], Zhuo Wang[1], & Robert J. Trapp[1]

[1]Department of Climate, Meteorology, & Atmospheric Sciences, University of Illinois Urbana-Champaign, Urbana, 61820, United States

Correspondence to: Zhuo Wang (zhuowang@illinois.edu)

Abstract: Tornado activity in the contiguous United States (CONUS) causes fatalities and financial losses every spring, motivating attempts to skillfully predict springtime tornadoes. Such predictions would facilitate decision-making and resource management for both public and private stakeholders. Using ERA5 reanalysis, we ~~identify~~analyze five April-May weather regimes (WRs) from 1981-2023, some of which strongly modulate tornado activity~~.~~, and the WR information is incorporated into a hybrid model to predict April-May CONUS tornado activity, including tornado outbreaks (days with >10 EF-1+ tornadoes). ECMWF seasonal forecasts initialized on April-1st are applied to predict WR frequency, including persistent and non-persistent WRs (lasting ≥5 and <5 consecutive days, respectively). ~~The WR information are incorporated into a hybrid model to predict April-May CONUS tornado activity, including tornado outbreaks (days with > 10 EF-1+ tornadoes).~~ Prediction skill is evaluated using leave-one-year-out cross-validation. Predicted and observed tornado outbreak frequencies are significantly correlated (cc=0.438). Outbreak predictions are more skillful during the positive phase of the Arctic Oscillation (AO) and Pacific North American pattern (PNA), with a proportion correct of 0.75 and 0.71, respectively. This implies that climate modes of low-frequency ~~climate modes~~variability can be used to identify forecasts of opportunity. SSTs over the North Pacific and North Atlantic may help explain the predictability of tornado activity but further work needs to be done to confirm those results. Our study demonstrates the potential for skillful prediction of spring tornado outbreaks using WR forecasts and should be prioritized in future work.

1. Introduction

Tornadoes in the contiguous United States (CONUS) result in significant losses of life and property ~~(Ashley 2007; Strader et al. 2024; NCEI 2024). From 1981-2023 there were 2833 tornado-related fatalities in the CONUS, accounting for ~13% of weather-related fatalities (National Weather Service 2025). Of these tornado-related fatalities, roughly 80% are associated with tornado outbreaks (TOs) (Schneider et al. 2004). Recent studies show a statistically significant increasing trend of +2.5 TOs per decade since 1960, the majority of which occur in the boreal spring (Graber et al. 2024; Brooks et al. 2014). Given these trends of tornado activity and their societal impacts, skillful seasonal predictions of springtime tornado activity would improve decision-making and resource management for both public and private stakeholders.~~ (Ashley, 2007; NCEI, 2024; Strader et al., 2024). From 1981-2023 there were 2833 tornado-related fatalities in the CONUS, accounting for ~13% of weather-related fatalities (National Weather Service, 2025). Of these tornado-related fatalities, roughly 76% are associated with tornado outbreaks (TOs; hereinafter, days with > 10 EF/F-1 tornadoes; Graber et al. 2025), consistent with Schneider et al. (2004). Recent studies show a statistically significant increasing trend of +2.5 TOs per decade since 1960, the majority of which occur in the boreal spring (Brooks et al., 2014; Graber et al., 2024). Given these trends of tornado activity and their societal impacts, skillful seasonal predictions of springtime tornado activity would improve decision-making and resource

Style Definition: Default Paragraph Font

Style Definition: Bibliography: Indent: Left: 0", First line: 0" management for both public and private stakeholders. ~~Subseasonal-to-seasonal (S2S) predictability of tornado activity has been previously investigated. Deterministic and probabilistic GEFS forecasts demonstrated skill in predicting tornado activity out to day 9 (Gensini and Tippett 2019). The Extended-Range Tornado Activity Forecast (ERTAF) project (Gensini et al. 2020) produced tercile-forecasts 2-3 weeks in advance during boreal spring and found predictive skill at both lead times. ERTAF emphasized the role of large-scale circulation patterns in conjunction with favorable severe thunderstorm environments, such as adequate convective available potential energy (CAPE) and vertical wind shear (VWS). Baggett et al. (2018) developed an empirical model using MJO phases and skillfully predicted weekly severe weather forecasts out 2-5 weeks in March-June. Similarly, Lepore et al. (2017) applied extended logistic regression based on the winter ENSO state to predict tornadoes in March-May, and found that the tornado prediction skill is higher during La Niña years compared to El Niño years. This background motivates the work herein that seeks to further explore skillful season prediction of tornado activity.~~

Subseasonal-to-seasonal (S2S) predictability of tornado activity has been previously investigated. Deterministic and probabilistic GEFS forecasts demonstrated skill in predicting tornado activity out to day 9 (Gensini and Tippett, 2019). The Extended-Range Tornado Activity Forecast (ERTAF) project (Gensini et al., 2020) produced tercile-forecasts 2-3 weeks in advance during boreal spring and found predictive skill at both lead times. ERTAF emphasized the role of large-scale circulation patterns in conjunction with favorable severe thunderstorm environments, such as adequate convective available potential energy (CAPE) and vertical wind shear (VWS). Baggett et al. ~~Low-frequency climate modes are important drivers of seasonal tornado activity and can serve as sources of their predictability. For example, La Niña (El Niño) winters tend to coincide with more (fewer) tornadoes in the winter (Cook and Schaefer 2008), and winter ENSO indices have been previously linked to springtime tornadoes (Allen et al. 2015; Lepore 2017). Lee et al. (2016) implied that springtime ENSO phase may be used to improve TO predictability, specifically. Across the CONUS, tornado activity during La Niña years peaks in mid-April, whereas activity during El Niño years peaks in late-May, when overall tornado frequency is greater than during La Niña (Allen et al. 2018). Furthermore, Tippett et al. (2022) found that a positive (negative) phase of the Arctic Oscillation (AO) coinciding with La Niña (El Niño) may increase (decrease) late winter and early spring tornado activity. The positive AO phase in winter and early spring on its own has been found associated with enhanced tornado activity (Childs et al. 2018; Niloufar et al. 2021; Tippett et al. 2022), while Elsner et al. (2016) found that the positive phase of the North Atlantic Oscillation (NAO) is linked to a decrease in springtime tornado activity in the Southeast. Additionally, the negative phase of the Pacific North American Pattern (PNA) is connected to a stronger Intra-Americas low-level jet and increased springtime tornado activity in the Midwest and Southeast (Munoz and Enfield 2011). Furthermore, positive sea surface temperatures (SST) anomalies in the Gulf of Mexico have been associated with increased tornado activity over the Southeast during the spring (Molina et al. 2016), and Chu et al. (2019) demonstrated the link between TOs and SST anomalies in April via a negative PNA pattern.~~

~~Though low-frequency climate modes provide an avenue for understanding the predictability of tornado activity~~(2018) developed an empirical model using Madden Julian Oscillation phases and skillfully predicted weekly severe weather forecasts out 2-5 weeks in March-June. Similarly, Lepore et al. (2017) applied extended logistic regression based on the winter El Niño Southern Oscillation (ENSO) phase to predict tornadoes in March-May, and found that the tornado prediction skill is higher during La Niña years compared to El Niño years. This background motivates the work herein that seeks to further explore skillful seasonal prediction of tornado activity.

Modes of climate variability are important drivers of seasonal tornado activity and can serve as sources of their predictability. Since tornado activity depends on favorable thermodynamic and dynamic environments (Thompson et al., 2003), shifts in jet streams or moisture transport associated with low-frequency climate variability may enhance or suppress springtime severe weather potential across the CONUS (Cook and Schaefer, 2008). A major mode of interannual climate variability is ENSO (Chen and Van den Dool, 1997), which is characterized by the anomalous warming (El Niño) and cooling (La Niña) of sea-surface temperatures (SSTs) in the central and eastern equatorial Pacific (Bjerknes, 1969). ENSO modulates the strength and position of the Pacific jet stream (Bjerknes, 1969) and can affect the large-scale circulations that influence the frequency, intensity, and spatial locations of CONUS severe weather. Previous studies have linked the winter ENSO phase to the variability of tornado activity (Allen et al., 2015, 2018; Cook and Schaefer, 2008; Knowles and Pielke, 2005; Lee et al., 2016).

The Arctic Oscillation (AO) and North Atlantic Oscillation (NAO) are prominent modes of climate variability in the extratropics (Cohen et al., 2014). Specifically, the AO refers to the leading EOF of variability in northern hemisphere sea-level pressures at mid and polar latitudes, while the NAO refers to the sea-level pressure difference between the Subtropical High and Subpolar Low over the North Atlantic (Hurrell, 1995; Hurrell and Deser, 2010; Thompson and Wallace, 2000; Wyburn-Powell and Jahn, 2024). NAO and AO are strongly correlated and modulate the strength and position of the midlatitude jet stream. Previous studies have linked the variability of NAO and AO to the variability of tornado activity, primarily over the central and eastern CONUS (Childs et al., 2018; Elsner et al., 2016; Niloufar et al., 2021; Tippett et al., 2022), suggesting that NAO and AO provide additional sources of predictability for springtime tornado activity.

Another important mode is the Pacific North American (PNA) pattern, which is a leading mode of low-frequency variability over the North Pacific and North America (Phillips et al., 2014). Although the PNA is influenced by ENSO (Wallace and Gutzler, 1981), it exhibits some independent variability (Li et al., 2019) and can exist in the absence of interannual SST variability (Lau, 1981). PNA modulates the position and intensity of the East Asian jet stream which influences large-scale circulations relevant for severe weather over the CONUS (Leathers et al., 1991; Li et al., 2019; Ning and Bradley, 2015). The negative phase of PNA has been associated with enhanced springtime tornado activity (Munoz and Enfield, 2011), and previous work has linked the variability of tornado activity to SST anomalies that are connected to PNA-like patterns over the Pacific (Chu et al., 2019). These relationships suggest that PNA, along with ENSO, AO, and NAO, potentially serve as sources of predictability for springtime tornado activity.

Since climate modes evolve on the seasonal and longer timescales, they may serve as sources of predictability for seasonal tornado activity. However, they do not fully capture the ~~day-to-day~~synoptic-scale variability of atmospheric circulation~~ patterns that drive weather. This gap can be filled by weather~~. Weather regimes (WRs~~).~~) can effectively bridge the gap. WRs represent a finite number of equilibrium, recurring states of the atmospheric circulation ~~(Michelangeli et al. 1995; Charney and DeVore 1979; Hannachi et al. 2017).~~(Charney and DeVore, 1979; Hannachi et al., 2017; Michelangeli et al., 1995). Miller et al. (2020) is among the first to apply WRs to tornado prediction. They constructed a hybrid prediction model for weekly tornado activity in May using WRs and achieved skillful prediction out to week 3. Tippett et al. (2024) explored the modulation of tornado activity using year-long WRs (Grams et al. 2017; Lee et al. 2023) and found statistically significant relations between tornado reports and WRs during all months except June-August, with results mainly driven by years with more Pacific Ridge WR days. Graber et al. (2025) identified two WRs that strongly affect the warm-season tornado activity, especially TOs, and developed an empirical model using WR frequency, persistence, and TD probabilities. The empirical model skillfully captures the interannual variability of both TDs and TOs using WR information derived from the ERA5 reanalysis and motivate its application to seasonal prediction.

The remainder of this paper is organized as follows. Section 2 describes the data and methodology, including the hybrid model. Section 3 presents the hybrid predictions and a discussion of the sources of predictability that help connect the WRs, tornado activity, and climate modes together. The paper will culminate with a summary and discussion in Section 4.

2. Methodology

2.1 Weather Regimes

~~Daily 500-hPa heights (500H) from the ERA5 reanalysis (Hersbach et al. 2020) were used to identify weather regimes (WRs) during April-May, the season of peak tornado activity (Graber et al. 2024), from 1981-2023. The seasonal cycle, defined as the long-term mean 500H for each calendar day, was removed from daily 500H. We used the WRs derived by Graber et al. (2025) using the K-means clustering method for 1960-2022 April-July as the reference WR patterns, and WRs were assigned by finding the reference WR pattern with the smallest Euclidean distance from the daily 500H anomalies. We took this approach because K-means clustering yields slightly different WR patterns in different time periods, and employing WRs during a longer time period as the reference patterns improves the robustness of the results.~~

~~Seasonal forecasts of daily 500H anomalies from the European Centre for Medium-Range Weather Forecasts (ECMWF) were used to predict April–May WR frequency from 1981-2023 (Vitart et al. 2017; Copernicus Climate Change Service 2018). The 25-ensemble forecasts are initialized once per month and are available on a $1^{\circ} \times 1^{\circ}$ grid. The forecasts initialized on April 1st were selected to mitigate the effect of the spring-predictability barrier (Duan and Wei 2012). WRs were assigned for each ensemble forecast by projecting the forecast 500H anomalies to the reference WR patterns, and the resultant long-term mean WR frequencies are similar to those derived from ERA5. Persistent and nonpersistent WRs are defined as WRs lasting for ≥5 consecutive days and for <5 consecutive days, respectively.~~

~~2.2 Tornado observations~~

~~Tornado reports during April-May 1981-2023 were obtained from the NOAA Storm Prediction Center Severe Weather Database. Reports are georeferenced with time, date, and EF/F rating. Tornado~~Daily 500-hPa heights (500H) from the European Centre for Medium-Range Weather Forecasts (ECMWF) reanalysis, version 5 (ERA5) (Hersbach et al., 2020) were used to analyze weather regimes (WRs) during April-May, the season of peak tornado activity (Graber et al., 2024), from 1981-2023. The seasonal cycle, defined as the long-term mean 500H for each calendar day, was removed from daily 500H. Unlike Graber et al. (2025), we did not remove the long-term linear trend in 500H of ERA5 to be consistent with the ECMWF seasonal forecast data. Rather than re-deriving WRs for this period, we used the WRs derived by Graber et al. (2025) using the K-means clustering method for 1960-2022 April-July as the reference WR patterns. WRs were assigned by finding the reference WR pattern with the smallest Euclidean distance from the daily

500H anomalies. We took this approach because K-means clustering yields slightly different WR patterns in different time periods and employing WRs during a longer time period as the reference patterns improves the robustness of the results.

Seasonal forecasts of daily 500H anomalies from the ECMWF were used to predict April−May WR frequency from 1981-2023 (Copernicus Climate Change Service, 2018; Vitart et al., 2017). The 25-ensemble forecasts are initialized once per month, are available on a 1° × 1° grid, are on 12-hour temporal resolution, and go out 7 months. The forecasts initialized on April 1st were selected to mitigate the effect of the spring-predictability barrier (Duan and Wei, 2012). WRs were assigned for each ensemble forecast by projecting the forecast 500H anomalies to the reference WR patterns, and the resultant long-term mean WR frequencies are similar to those derived from ERA5. Persistent and nonpersistent WRs are defined as WRs lasting for ≥5 consecutive days and for <5 consecutive days, respectively.

2.2 Tornado observations

Tornado reports during April-May 1981-2023 were obtained from the NOAA Storm Prediction Center Severe Weather Database. Reports are georeferenced with time, date, and EF/F rating. To be consistent with previous work, tornado days (TDs) are defined as days with ≥1 tornadoes ranked EF/F-1 or greater, and tornado outbreaks (TOs) are defined as any day with >10 tornadoes ranked EF/F-1 or greater ~~(Graber et al. 2024, 2025).~~(Graber et al., 2024, 2025). EF/F-0 reports were excluded due to reporting uncertainties ~~(Brooks et al. 2014; Trapp 2013).~~(Brooks et al., 2014; Trapp, 2013). Known biases remain in this database, which a focus on TDs rather than raw tornado reports attempts to alleviate ~~(Brooks et al. 2014; Trapp 2014; Graber et al. 2024).~~(Brooks et al., 2014; Graber et al., 2024; Trapp, 2014).

2.3 Hybrid model

Following Graber et al. (2025), an empirical model was used to evaluate the seasonal prediction of tornado activity:

$$\boldsymbol{TI}(\boldsymbol{t}) = \sum_{\boldsymbol{i}=\boldsymbol{1}}^{\boldsymbol{5}} \boldsymbol{f}(\boldsymbol{i},\boldsymbol{t})_{\boldsymbol{p}} \times \boldsymbol{P}_{\boldsymbol{i},\boldsymbol{p}} + \sum_{\boldsymbol{i}=\boldsymbol{1}}^{\boldsymbol{5}} \boldsymbol{f}(\boldsymbol{i},\boldsymbol{t})_{\boldsymbol{np}} \times \boldsymbol{P}_{\boldsymbol{i},\boldsymbol{np}} \qquad \textbf{(1)}$$

where P_i denotes the TD probability for each WR, which is defined as the number of TDs with WR-i divided by the number of total WR-i days. The predictand tornado index for year t, $TI(t)$, is computed by the seasonal count of WR-i days in year t, $f(i,t)$, multiplied by P_i. TD probabilities and counts were calculated for persistent and nonpersistent WRs separately, denoted by subscripts p and np, respectively. ~~The same procedure was applied to TOs (Graber et al. 2025).~~The same procedure was applied to TOs.

To evaluate tornado prediction skill, a leave-one-year-out cross-validation method was employed. Specifically, 1981 was first held for testing, and $P_{i,np}$ and $P_{i,p}$ were determined using the WR information derived from the ERA5 reanalysis and tornado reports during 1982-2023. The seasonal WR counts from the ECMWF ensemble forecasts for 1981 were used in Eq. 1 to predict the ~~TI~~tornado index value in 1981. This process was repeated for each year, yielding a predicted time series of ~~TI.~~the tornado index. The ~~TI~~tornado index time series for all ensemble members were averaged to form the ensemble mean ~~TI~~of tornado index, which was standardized using z-score normalization.

The prediction skill was quantified using the Pearson correlation between the predicted and observed ~~TI~~tornado index time series. Additionally, a three-tier categorical verification was used by classifying both observed and predicted ~~TI~~tornado index values into lower, middle, and upper terciles. A correct prediction was recorded when the observed and predicted ~~TI~~tornado index values fell within the same tercile for a given year. The proportion correct (PC) is defined as the number of correct predictions divided by the number of total predictions.

To assess the potential impacts of climate modes on tornado predictability, PC was calculated separately for positive, negative, and neutral phases of various low-frequency climate modes (see more information on climate modes in section 2.4). Significance ($p \leq 0.05$) between PC of each phase and random chance (33% for three-tier verification) was determined using a Monte Carlo test with 10,000 resamples.

2.4 Sources of Predictability

The impacts of some ~~low-frequency~~ climate modes, ENSO (via Nino3.4), PNA, NAO, and AO, on tornado activity and WR counts were investigated to provide a physical basis for TD and TO predictability. ~~Indices of ENSO (via ENSO3.4), PNA, NAO, and AO were downloaded~~We focus on their low-frequency variability on the seasonal and longer time scales and derived their April-May seasonal indices using the data from the NOAA Climate Prediction Center ~~(2024a,b).~~(2024b, a). Positive and negative phases of a climate mode are defined as the years when the standardized springtime (April-May) index exceeded ± 0.9. 0.9 was used instead of 1.0 to slightly increase the sample size.

TD and TO probability anomalies were calculated for each climate mode phase as:

$$\boldsymbol{P_a = \frac{P_r - P_c}{P_c} \times 100\%} \qquad \textbf{(2)}$$

where the climatological mean TD (TO) probability (P_c) is defined as the total number of TDs (TOs) divided by the total number of days; P_r is TD (TO) probability for the given phase of the climate mode; and P_a is the percentage anomaly.

3. Results

3.1 Model Prediction

For completeness, the five WRs (Fig. 1a-e) are briefly described here. WR-A features anomalous highs over ~~both~~ the ~~eastern~~Pacific Northwest and ~~western~~off the U.S. ~~coasts~~east coast. WR-B is characterized by a prevailing anomalous low centered over central North America and an anomalous high over the Southeast ~~CONUS~~. WR-C exhibits a three-cell wave pattern with anomalous lows over both coasts. WR-D and WR-E display west-east dipole patterns that nearly mirror each other. The WR spatial structures closely resemble WRs in Miller et al. (2020), Zhang et al. (2024), and Lee et al. (2023). Specifically, WR-A and WR-E resemble the Pacific Ridge and Alaskan Ridge regimes in Lee et al. (2023), respectively, but noticeable differences exist due to differences in data processing procedures and the time periods analyzed. The impacts of the WRs on CONUS tornado activity ~~in the CONUS~~ during April-May 1981-2023 (Fig. 1f and 1h) are similar to those during April-July 1960-2022 from Graber et al. (2025; their Fig. 4). WR-A is the least favorable WR for springtime tornado activity, and WR-B is the most favorable. Tornado activity in WR-C and WR-E are slightly unfavorable, and in WR-D is slightly favorable. The estimated TDs and TOs based on the empirical model (Eq. 1) and the ERA5 during April-May 1981-2023 are significantly correlated with the observed time series (Figs. 1g and 1i).

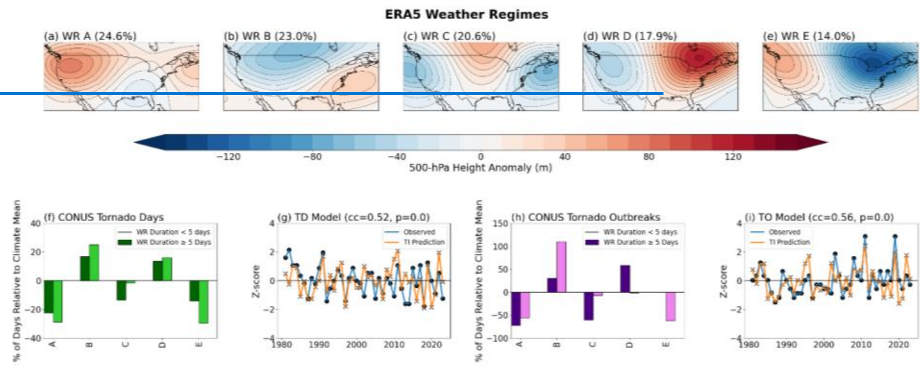

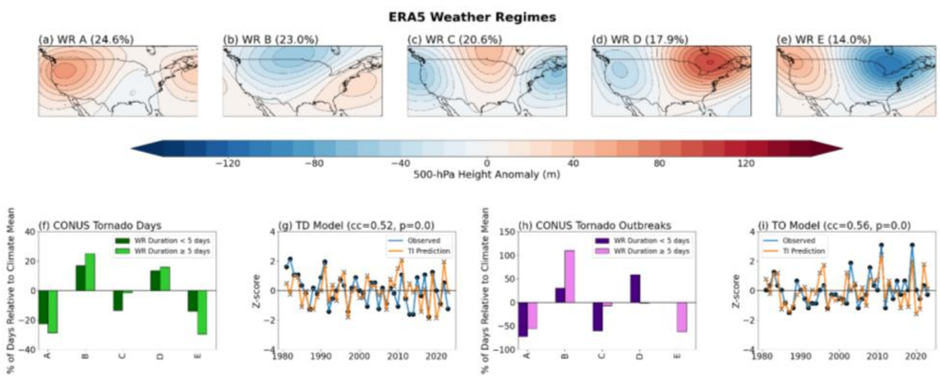

Figure 1: 500H anomaly patterns of WRs A-E with long-term frequency indicated in panel title (a-e). ERA5 tornado day (f) and tornado outbreak (h) CONUS probability anomalies for persistent ($\geq$ 5 days; light green, pink) and nonpersistent (< 5 days; dark green, indigo) WRs. Time series of standardized tornado days (g) and tornado outbreak days (i) from the observation (blue) and estimation of the empirical ~~model~~ modeling (red). Spearman rank correlation and p-value are indicated in panels g and i.

Before assessing the hybrid predictions of tornado activity, we first evaluate the prediction skill of WRs by the ECMWF springtime forecasts. The ECMWF ensemble mean prediction of springtime WR counts are significantly correlated with the ERA5 springtime WR counts (Fig. 2a-e). This indicates the seasonal predictability of WRs and provides the basis for tornado prediction using the hybrid framework (i.e., Eq. 1).

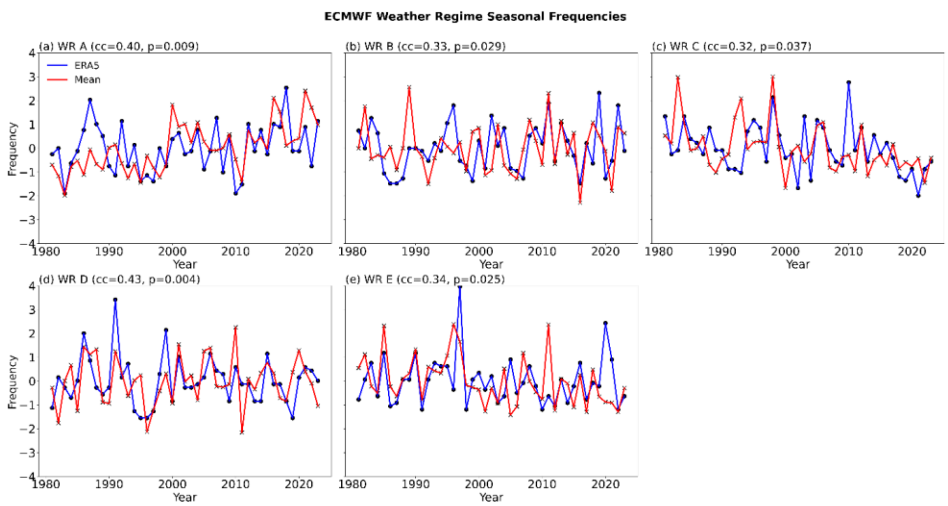

Figure 2: Z-score normalized ERA5 (blue) and ECMWF ensemble mean (red) springtime frequency of each WR with Spearman rank correlation and p-value indicated in each panel (a-e).

We assess the hybrid predictions of TDs and TOs using leave-one-year-out cross-validation method (Fig. ~~3a-b~~3). The hybrid prediction of TOs has a significant Pearson correlation of **0.38** with the observed TO time series, while TD prediction shows no skill, with a Pearson correlation close to zero. The skill contrast between the TO and TD predictions is probably because TOs usually occur under strong and persistent synoptic-scale patterns (Mercer et al. 2012; Cwik et al. 2022; Jiang et al. 2025; Graber et al. 2025), while ~~some~~ transient, and weak ~~WR days~~patterns, which are not well captured by the ECMWF springtime forecasts, may have strong impacts on TDs. In addition, it is worth noting that the percentage anomalies of TOs associated with various WRs are generally stronger than those of TDs (Fig. 1).

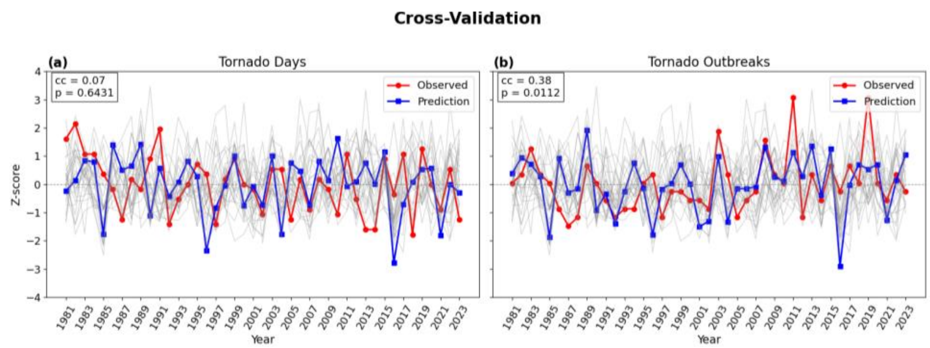

Figure 3: Standardized TDs (a) and TOs (b) time series from observation (red) and the hybrid prediction (blue). Thin gray lines represent the individual ensemble prediction (grey) time series. Pearson correlations (cc) and p-values (p) are shown at the upper left corner of each panel.

The tercile-based TO prediction indicates that the hybrid model correctly predicts **53.5%** of years. Additionally, the PC is strongly modulated by some climate modes (Fig. 4). In particular, the hybrid model performs significantly better during the positive phases of the AO (**75%** of correct prediction), NAO (**71.4%**), PNA (**71.4%)**, and ENSO (**70.0%)**. PC also improves in the negative phases of NAO (**62.5%)**, AO (**55.6%)**, and ENSO (**55.6%**), but the increases in PC are not significant ($p > 0.05$). In contrast, the PC in a neutral phase is below **53.5%**. Although the PC of the tercile-based TD prediction is close to random chance (**34.9%**), the hybrid model performs better in +PNA years (**57.1%,** p=0.23) (figure not shown). This suggests that climate modes may be used to identify forecasts of opportunity for springtime tornado prediction.

Additional cross-validation tests by leaving two-, three-, four-, and six-year out yield similar results (Fig. S1). TO predictions maintain skillful across all tests, while TD predictions remain unskillful.

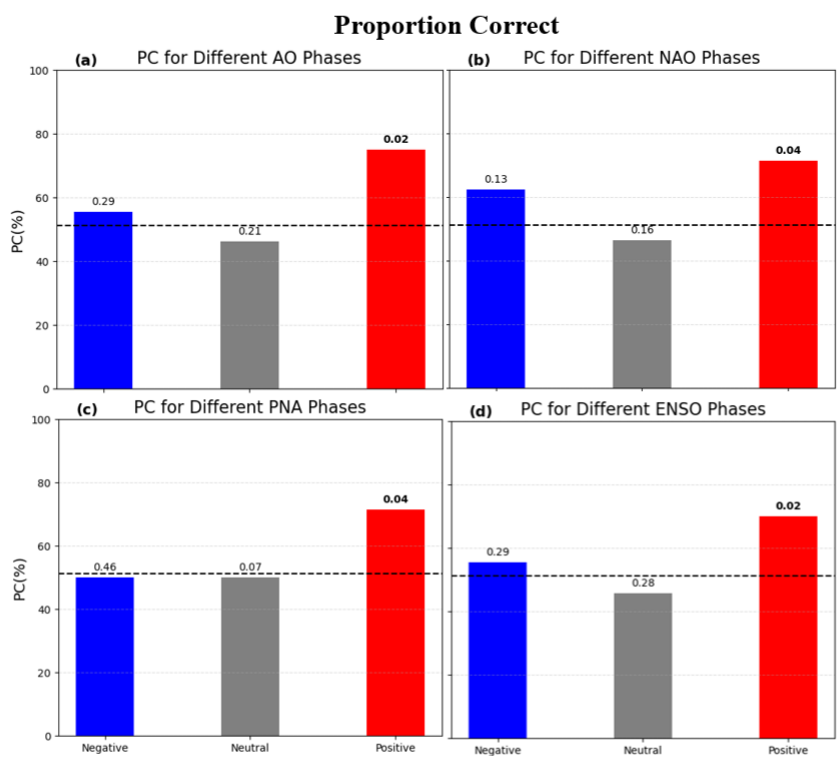

Figure 4: Proportion of correct TO predictions for negative (blue), neutral (grey), and positive (red) phases of AO (a) and NAO (b), PNA (c), and ENSO (d). Numbers above the bars represent p-values using a Monte Carlo test with 10,000 resamples, and bold values represent significant ($p \leq 0.05$) differences from random chance. The dashed, horizontal line represents the overall PC (i.e., 53.5%).

3.2 Low-frequency climate modes as sources of Predictability

To investigate predictability sources for tornado activity, the relationship between tornado activity and low-frequency climate modes is examined using springtime TD and TO probability anomalies associated with the AO, NAO, PNA, and ENSO phases (Figs. 5a-h). In addition to CONUS, we examined different regions, Midwest (MW), Southern Great Plains (SGP), Southeast (SE), and Southern Great Plains (SGP) (Fig. S2). The region definitions follow Moore (2018), with exception of the SGP, which herein contains New Mexico because it has storm events similar to those in the Texas Panhandle.

Significantly enhanced TO probability in the CONUS and Midwest is associated with the -AO phase. TO probability is also enhanced in the SE, NGP and SGP, but the anomalies are not statistically significant. In contrast, the probability anomalies of TDs during +AO and -AO phases are much weaker and all are statistically insignificant, consistent with Tippett et al. (2022) showing a weaker tornado-AO relationship in April than in February. +AO years are characterized by an anomalous high over the southeastern CONUS and negative anomalies over the north-central CONUS (Fig. ~~S2a~~S3a), implying enhanced westerly flow aloft and promoting moisture and warm-air advection from the Gulf of Mexico. These circulation anomalies lead to positive MUCAPE and ~~TD~~TO probability anomalies over the Southeast and SGP (Fig. ~~S2a~~S3a). In contrast, -AO years feature negative 500H anomalies over the central CONUS, accompanied by anomalously positive VWS. ~~Although anomalously low MUCAPE during -AO years tends to suppresses TD probability, the enhanced VWS supports anomalously positive TO probability anomalies (Sherburn et al. 2016).~~Although reduced MUCAPE tends to suppress TD probability, the increased VWS supports positive TO probability anomalies when it occurs on days where MUCAPE is high (Diffenbaugh et al., 2013; Sherburn et al., 2016). These positive TO probability anomalies during -AO are only statistically significant over the Midwest, consistent with the region of anomalously positive VWS anomalies.

The TD and TO probability anomalies during the NAO phases are generally consistent in sign with those during AO phases when one phase is statistically significant, but quantitative differences exist. TD probability is reduced significantly over CONUS, SGP, and NGP, and TO probability is reduced significantly over NGP during the +NAO phase. +NAO years feature an anomalous 500H high over the west-central CONUS, which hinders moisture and heat transport from the Gulf of Mexico. These circulation changes result in anomalously low ~~MUCAPE and~~ TD probabilities over the SGP and NGP (Fig. ~~S2e~~S3e). Additionally, anomalously low VWS over the SGP further limits tornado potential during +NAO years. However, +NAO years also feature an anomalous 500H high over the western Atlantic and anomalous 500H low over the Southeast, which enhances southerly flow and moisture transport into the Southeast ~~(Zhao et al. 2025), supporting positive MUCAPE anomalies (Fig. S2e) and corresponding positive TO probability anomalies in that region (Fig. 5~~(Zhao et al., 2025), supporting positive MUCAPE anomalies (Fig. S3e) and corresponding positive TO probability anomalies in that region (Fig. 5d).

The positive PNA phase (+PNA) is unfavorable for tornado activity across the CONUS, MW, SGP, and SW, particularly for TOs (Fig. 5f). +PNA years feature an anomalous 500H high over the western CONUS and an anomalous 500H low over the eastern CONUS (Fig. ~~S2c~~S3c), implying reduced moisture transport from the Gulf of Mexico and anomalously low VWS. These circulation anomalies hinder tornado activity across the MW, SGP, and SW. Springtime PNA has become more negative over time (Fig. ~~S3~~S4), possibly explaining the increasing trend in TOs ~~(Graber et al. 2024), though further work with other seasons needs to be done to confirm~~

~~this.~~(Graber et al., 2024), though further work with other seasons needs to be done to confirm this, which goes beyond the scope of this study.

TO probability is enhanced in La Nina years in various regions, although the enhancement is significant only in the SE. Additionally, TD probability over the SGP and TO probability over NGP are enhanced in El Nino years. The La Nina-tornado-activity link is largely consistent with previous work (e.g., Cook and Schaefer 2008; Cook et al. 2017; Tippett et al. 2022; Allen et al. 2015; Moore 2019), but it is worth noting that the ENSO state in the spring time is examined here, while some previous studies focus on the winter ENSO state. Previous studies have found that ENSO modulates the phase of PNA during boreal winter (Li et al., 2019; Soulard et al., 2019); however, these spring results are not consistent with those findings. Accordingly, the correlation between the ENSO and PNA indices are much stronger during the peak stage of ENSO in December than during the ENSO decay stage in April-May (Fig. S5).

Formatted: Not Strikethrough

The model appears to perform better (Fig. 4) in years when climate modes unfavorable for TOs, such as +NAO and +PNA, are present. To further evaluate skill, the Threat Score (Schaefer, 1990) was calculated for upper-tercile TO years. These years yield a Threat Score of **0.375** with 6 hits, 2 misses, and 8 false alarms, indicating a tendency for the model to overpredict TOs. For lower-tercile years, the Threat Score is slightly higher at **0.429**, with 9 hits, 7 misses, and 5 false alarms. While lower-tercile years have greater overall skill, they also include more misses. Overall, the model demonstrates higher skill for lower-tercile years, and modest skill for upper-tercile years.

Overall, the link between climate modes and tornado activity suggests that low-frequency climate modes provide a source of predictability for springtime tornado prediction~~.~~, but the predictability seems slightly higher during inactive years for tornado activity. Additionally, low-frequency climate modes modulate TO probabilities more strongly than TD probabilities, consistent with the stronger TO anomalies associated with WRs (Fig. 1h) and the higher predictive skill of TOs (Fig. 3).

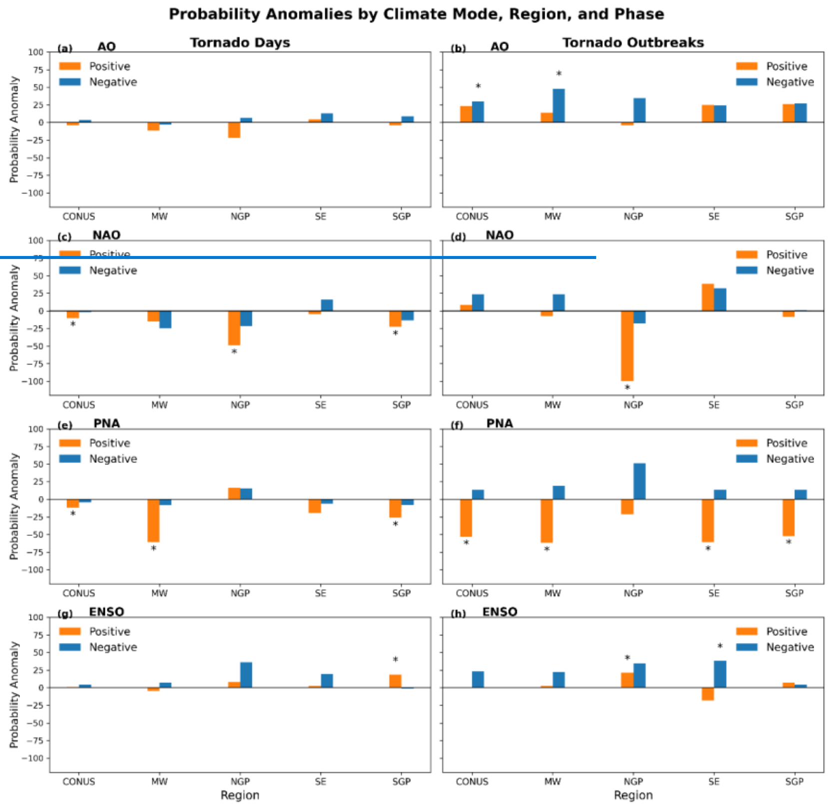
Probability Anomalies by Climate Mode, Region, and Phase
Tornado Days
Tornado Outbreaks
(a) AO
(b) AO
(c) NAO
(d) NAO
(e) PNA
(f) PNA
(g) ENSO
(h) ENSO
Positive
Negative
Probability Anomaly
CONUS
MW
NGP
SE
SGP
Region

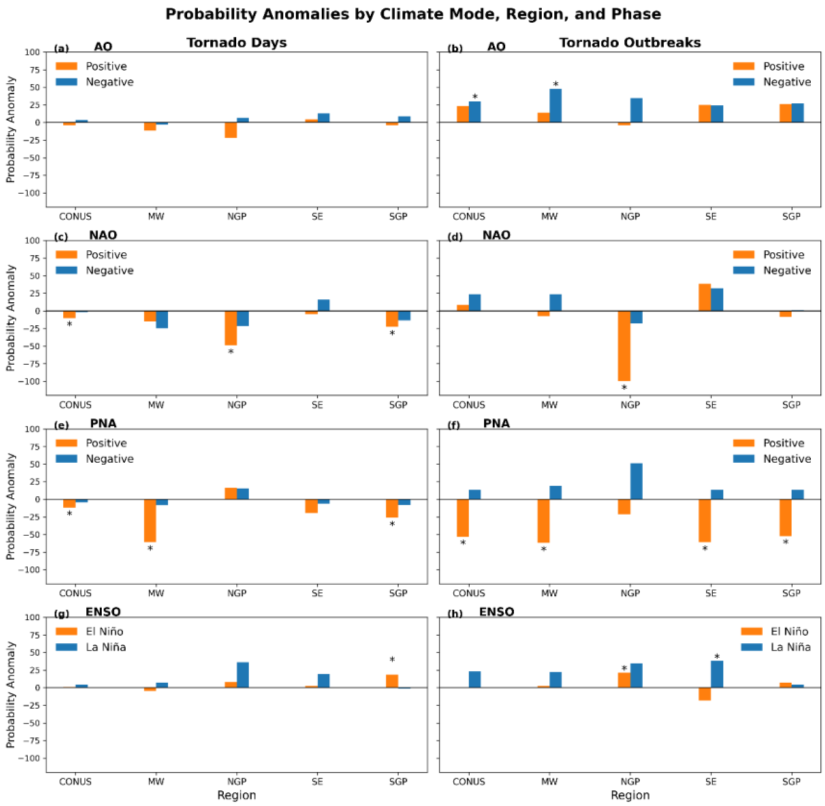

Figure 5: TD (left column) and TO (right column) probability anomalies by region and climate mode: AO (a-b), NAO (c-d), PNA (e-f), and ENSO (g-h). Asterisks represent significant anomalies ($p \leq 0.05$) based on a Monte Carlo test with 10,000 resamples of each regions' data.

The connection between climate modes and WRs is examined next to investigate whether climate modes modulate tornado activity via WRs. Figure 6 shows the frequency of WRs in different phases of low-frequency climate modes, which is defined as the number of WR days during a given phase of the climate mode divided by the total number of days in that phase. The frequency of WR-A is only ~**15%** during the -AO phase, while the frequency of WR-B is ~**33%** (Fig. 6). The increased occurrence of WR-B and decreased occurrence of WR-A in -AO years compared to the long-term mean (Fig. 1) are consistent with the positive TO probability anomalies in the CONUS and Midwest during the -AO years (Fig. 5).

During +NAO years, WR-A occurs on approximately **35%** of days, making it the dominant WR during this phase. This predominance of WR-A is consistent with the reduced TD probability in the CONUS, NGP, and SGP, and reduced TO probability in the NGP during NAO+ years (Fig. 6).

Composite 500H anomalies for +NAO years resemble WR-A, while composite 500H anomalies for +AO show a mix of WR-A and WR-B (Fig. ~~S2~~S3).

During +PNA years, WR-B occurs on ~**15%** of days, whereas WR-E occurs on ~**25%** of days, making it the most frequent WR during this phase (Fig. 6). The reduced occurrence of WR-B and increased occurrence of WR-E are consistent with reduced TD and TO activity over CONUS, MW, and SGP during +PNA (Fig. 5). Composite 500H anomalies during +PNA years resembles WR-E, with an anomalous high over the western CONUS and an anomalous low over the eastern CONUS (Fig. ~~S2c~~S3c).

Neither positive nor negative phase of ENSO is associated with significant changes in WR-A or WR-B frequency. Instead, the frequency of WR-C is reduced significantly in both phases of ENSO, and WR-E occurs more frequently in the positive phase of ENSO, which is consistent with the reduced tornado activity during El Nino years reported in previous studies ~~(Cook et al. 2017).~~(Cook et al., 2017). Relative to the neutral phase, WR-E also occurs more frequently during the negative phase of ENSO, which is statistically significant. However, WR-E's occurrence during the negative phase of ENSO is still less than any other WR.

To summarize, WRs associated with increased springtime tornado activity ~~tend to~~ occur more frequently during the climate mode phases that favor increased tornado activity, while WRs associated with suppressed tornado activity preferentially occur during climate mode phases that are unfavorable for tornado activity. These consistent relationships provide additional confidence in the robustness of the WR-based prediction framework and help to understand ~~tornado~~the predictability of tornado activity.

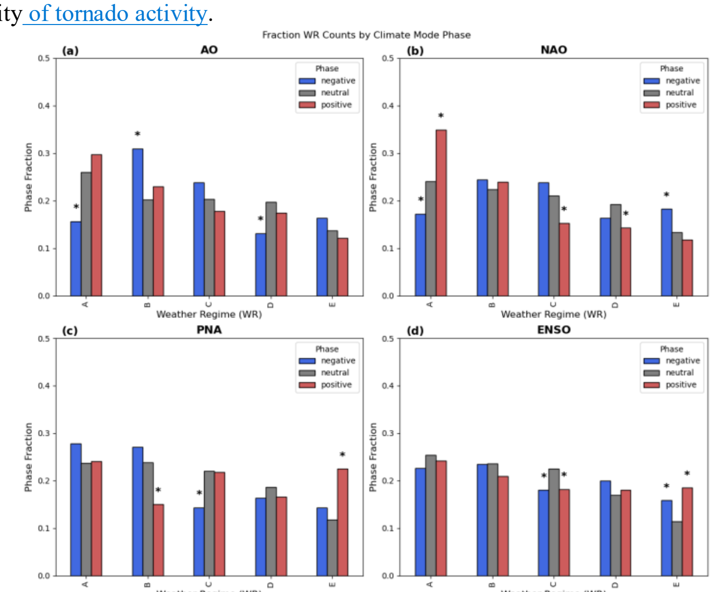

Figure 6: WR frequencies in different phases of AO (a), NAO (b), PNA (c), and ENSO (d). An asterisks indicates that the frequency is significantly different ($p \leq 0.05$) from that during the corresponding neutral phase via a student t-test.

3.3 Possible role of SST

In addition to low-frequency climate modes, slowly-evolving ~~SST may~~SSTs can also ~~serve as~~be an important source of predictability~~.~~, sometimes through their coupling with these modes. The ~~connection between SSTs, large-scale circulations, and tornado activity~~role of SSTs is further examined in Fig. 7. Extended Range SST (ERSST) ~~(Huang et al. 2017)~~(Huang et al., 2017) of 2° x 2° resolution is used here, and we focus on the month of April because SST signals in April are more pronounced than in May based on a previous study ~~(Chu et al. 2019)~~(Chu et al., 2019) and our own analysis. In addition, the analysis is done for 1960-2023 to increase the sample size. For each WR, active and inactive regime years are ~~identified~~defined as the years when the springtime WR count ~~of the WR~~ exceeds $\pm$ 1 standard deviation from the mean, and composite anomalies of SST and 500H are constructed for these active and inactive years of the WR.

+WR-A years are characterized by an anomalous 500H high over the north-central CONUS, as part of a well-defined wavetrain pattern extending from the North Pacific to southern Greenland, in addition to an anomalous low over the Southeast and Gulf of Mexico. Although there are coherent cold and warm SST anomalies associated with the anomalous low and high over the North Pacific, respectively, the SST anomalies are not significant. Significant SST anomalies exist over the North Atlantic associated with anomalous 500H high. In contrast, the -WR-A years feature an anomalous low over the central CONUS, nearly opposite to the +WR years. However, the anomalous circulation patterns over the North Pacific and North Atlantic are not a simple mirror image to those during +WR-A years. The anomalous 500H field is characterized by an elongated anomalous low over the midlatitude North Pacific and North Atlantic, reminiscent of the -AO pattern. Significant SST anomalies are found over the North Pacific and North Atlantic, resembling the Atlantic tripole SST pattern, which helps to maintain the NAO pattern via positive air-sea interaction ~~(Czaja and Frankignoul 2002).~~(Czaja and Frankignoul, 2002). Consistent with this circulation, WR-A is suppressed during -NAO and -AO years (Fig. 6).

WR-B is most favorable for tornado activity over the CONUS. Though positive SST anomalies exist over the central Pacific in +WR-B years, consistent with that shown in Chu et al. (2019) for April tornadoes, the anomalies are not significant. The 500H pattern over the North Atlantic is reminiscent of a -AO pattern, consistent with increased WR-B occurrence during -AO (Fig. 6). Significant, negative SST anomalies exist over the North Pacific in -WR-B years. The associated North Pacific negative SSTs and the 500H high over Canada are reminiscent of a +PNA pattern, consistent with reduced WR-B occurrence during +PNA (Fig. 6). Though statistically insignificant, the warm SST anomalies in the northern Pacific during +WR-B have been previously linked to enhanced CONUS tornado activity ~~(Zhao et al. 2025)~~(Zhao et al., 2025) through a weakening and eastward shift of the Aleutian Low (Chu et al~~.~~., 2019), which promotes enhanced southerly flow of moisture and heat from the Gulf of Mexico.

~~+WR-C years feature anomalously cold SSTs in the midlatitude North Pacific and North Atlantic as well as in the Gulf of Mexico. The cold SST anomalies over the Gulf of Mexico may limit moisture availability (Molina et al. 2016)~~+WR-C years feature anomalously cold SSTs in the midlatitude North Pacific and North Atlantic as well as in the Gulf of Mexico. The cold SST anomalies over the Gulf of Mexico may limit moisture availability (Molina et al., 2016), partially offsetting the otherwise favorable southerly 500H anomalies over the central US. This compensating thermodynamical and dynamical effects help explain the near-climatological tornado activity during WR-C (Fig. 1f, h). In contrast, -WR-C years are associated with prevailing

Field Code Changed

warm SST anomalies in the North Pacific. Significant SST anomalies, however, are confined to the subtropical North Atlantic and portions of the subtropical eastern Pacific.

+WR-D and +WR-E years feature anomalously warm and cold SSTs in the Gulf of Mexico, respectively, though these anomalies are not statistically significant. Over the subtropical western and central North Pacific, respectively, +WR-D years exhibit significant warm SST anomalies, while +WR-E years show significant cold SST anomalies. Given that WR-D and WR-E are linked to enhanced and reduced TD probability, respectively (Fig. 1), this suggests that SST anomalies in the subtropical Pacific may be a source of predictability for tornado activity over the CONUS. However, the robustness of this relationship requires further examination given the ~~patchy~~incoherent pattern of the significant SST signals, and the underlying mechanisms also need to be investigated. In addition, significant cold SST anomalies exist over the North Atlantic for +WR-E years, suggesting cold SSTs in this region may be associated with reduced TD probabilities over the CONUS.

We also examined the composite SST and 500H anomalies for active and inactive TO years (Fig. S6). Interestingly, significant SST anomalies are found over equatorial eastern Pacific, North Pacific, and subtropical western North Atlantic during inactive TO years, while significant SST anomalies are nearly absent during active TO years. The lack of significant SST anomalies in the active tornado years are consistent with the relatively limited SST signals during the active WR-B and WR-D years and during the inactive WR-A and WR-E years, and it helps to explain the higher predictability of inactive tornado years discussed in the previous section.

Overall, Fig. 7 suggests that SST anomalies over the North Pacific and North Atlantic may help explain the predictability of some WRs and thus the predictability of tornado activity within the hybrid framework. However, WR-B and WR-D, which favor tornado activity over the CONUS (Fig. 1), are not associated with many coherent, statistically significant SST anomalies. Further investigation using longer observational records and focusing on different seasons is needed to better understand the predictability—or lack thereof—of tornado activity.

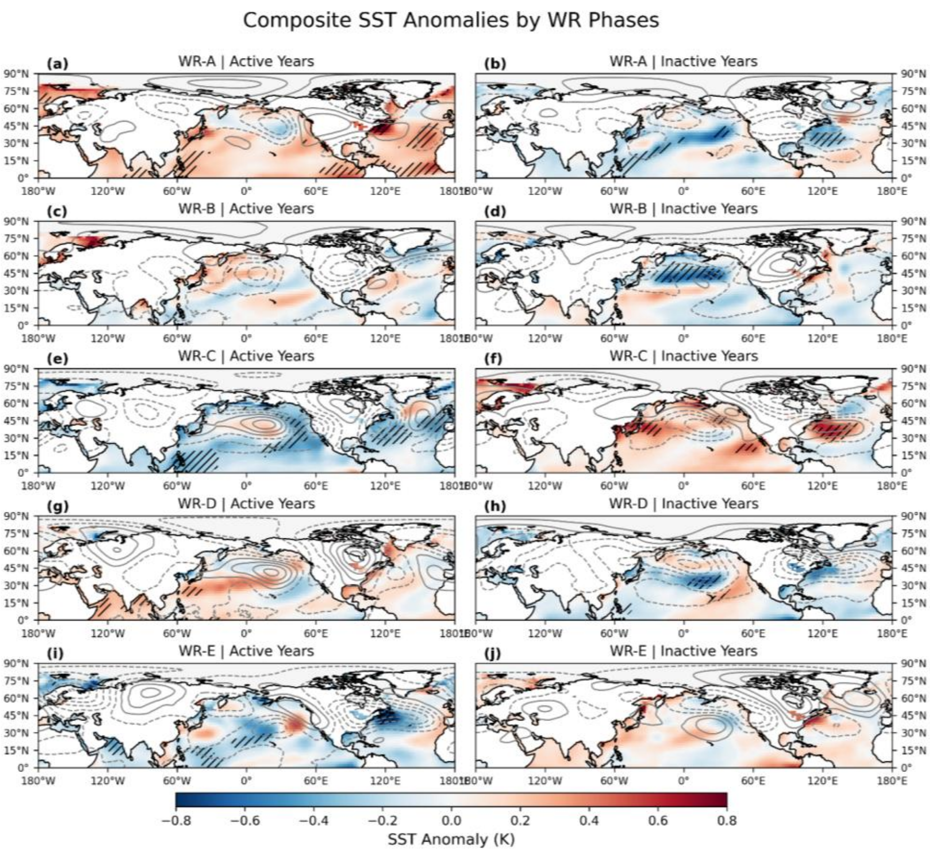

Figure 7: April SST anomalies for active and inactive WR years, and hatching indicates significant SST anomalies ($p \leq 0.05$) using a one-sample, two-sided t-test. 500H anomalies are shown in ~~black~~gray contours.

4. Summary

A hybrid model for the seasonal prediction of CONUS springtime tornado activity is evaluated during 1981-2023. The model employs WR forecasts from the ECMWF ensemble springtime forecasts initialized on April-1st. Using the leave-one-year-out cross-validation, the WR-based model shows no predictive skill for TDs, but the predicted time series of TO days is significantly correlated with the observed time series. Predictive skill for TOs is modulated by low-frequency climate modes and is significantly enhanced during +AO, +NAO, +PNA, and El Niño years, with the proportion correct of 75%, 71.4%, 71.4%, and 70%, respectively. Given the difficulty of predicting TDs beyond subseasonal timescales ~~(Gensini et al. 2020)~~(Gensini et al., 2020), springtime prediction efforts should prioritize TOs due to their higher predictive skill and societal impacts, and low-frequency climate modes can help to identify forecasts of opportunity.

To investigate the predictability sources of springtime tornado activity, the composite TD and TO probability anomalies were examined during different phases of climate modes. Significantly enhanced TO probability anomalies were associated with -AO and La Niña years, while significantly reduced TO probability anomalies were associated with +NAO and +PNA years. Corresponding circulation patterns during these years provide physical support, through CAPE and vertical shear anomalies. TO probability anomalies are generally stronger than TD anomalies associated with climate modes, which helps explain the higher predictive skill of TOs. These results suggest that the model performs better during years that are unfavorable for tornado activity, possibly due to a lower signal-to-noise ratio, and use of the Threat Score confirms the model is better in inactive TO years. However, this skill test still demonstrates modest skill in active TO years.

Additionally, WR occurrence is modulated by some climate modes. WR-A is the dominant WR during +NAO years and WR-E is the dominant WR during +PNA years, consistent with reduced tornado activity during +NAO and +PNA years. Furthermore, WR-B is the dominant WR during -AO years and is the least frequent WR during +PNA years, consistent with enhanced (reduced) tornado activity during the -AO (+PNA) phase. WRs associated with increased springtime tornado activity tend to occur more frequently during the climate mode phases that favor increased tornado activity, while WRs associated with suppressed tornado activity preferentially occur during climate mode phases that are unfavorable for tornado activity. This physical consistency supports the use of WRs as a physically meaningful framework for predicting TOs.

The role of SSTs in the predictability of WRs (with implication for the predictability of tornado activity) was examined, with the focus on April SST anomalies. -WR-A years feature a -NAO SST and 500H pattern over the North Atlantic, consistent with WR-A being suppressed during -NAO patterns. +WR-B years feature positive, though statistically insignificant, SSTs over the central Pacific consistent with patterns shown in Chu et al. (2019) for April tornadoes. In addition, significantly negative SST anomalies exist over the northern Pacific during -WR-B years, consistent with suppressed WR-B and TO during +PNA years. Overall, SST anomalies can help explain WR predictability, but SST signals for some WRs are statistically insignificant or ~~patchy~~incoherent, making it challenging to identify specific SST-based predictors for WRs or tornado activity. Further investigation based on longer observational records would help better understand the role of SST in the predictability of WRs and tornado activity.

This study demonstrates that skillful prediction of springtime TOs is indeed possible with current resources via the connection between tornado activity and WRs. Questions remain on whether SSTs are a reliable driver of springtime TOs as well as the temporal extent to which TOs can be predicted.

Code Availability

Important python files for WR identification and modeling are included at the following link:

https://github.com/Matt0604/Springtime-Prediction-Manuscript

Formatted: Font: +Body (Calibri), 11 pt

Data Availability

The ERA5 data are available through the NCAR research data archive (RDA) (d633000) and the Copernicus Climate Data Store (CDS):

https://doi.org/10.24381/cds.bd0915c6 (Hersbach et al~~.~~., 2023a)

Field Code Changed

https://doi.org/10.24381/cds.adbb2d47~~(Hersbach et al. 2023b)~~(Hersbach et al., 2023b)

The ECMWF data are available through the Copernicus Climate Data Store (CDS):

https://doi.org/10.24381/cds.50ed0a73 ~~(Copernicus Climate Change Service 2018)~~

(Copernicus Climate Change Service, 2018)

April SST data are available through the Extended-range sea surface temperatures data ~~(Huang et al. 2017)~~(Huang et al., 2017).

The tornado report data used in this study are available through the NOAA Storm Prediction Center severe weather database:

https://www.spc.noaa.gov/wcm/#data

Author Contributions

Conceptualization: MG, ZW, RJT

Methodology: MG, ZW, RJT

Project Administration: ZW, RJT

Supervision: ZW, RJT

Writing – Original Draft: MG

Writing – Review and Edits: MG, ZW, RJT

Competing Interests

Authors declare they have no competing interest.

Acknowledgements

We acknowledge the NCAR Computation and Information Systems Laboratory (CISL) for providing computing resources through Derecho. All ERA5 data used in this study are available at the research data archive. All ECMWF seasonal forecast data are available via the Copernicus Climate Change Service. Tornado report data are available through the NOAA Storm Prediction Center severe weather database.

References

Allen, J. T., ~~M. K.~~ Tippett, M. K., and ~~A. H.~~ Sobel, ~~2015:~~A. H.: Influence of the El Nino/Southern Oscillation on tornado and hail frequency in the United States~~.~~, Nat. Geosci., 8, 278–283, https://doi.org/10.1038/ngeo2385, 2015.

~~———, M.~~Allen, J. T., Molina, M. J., and ~~V. A.~~ Gensini, ~~2018:~~V. A.: Modulation of annual cycle of tornadoes by El-Nino-Southern Oscillation~~.~~, Geophys. Res. Lett., 45, 5708–5717, https://doi.org/10.1029/2018GL077482, 2018.

Ashley, W. S~~., 2007:~~.: Spatial and temporal analysis of tornado fatalities in the United States: 1880-2005~~.~~, Weather Forecast., 22, 1214–1228, https://doi.org/10.1175/2007WAF2007004.1, 2007.

Bjerknes, J.: Atmospheric Teleconnections from the equatorial Pacific, Mon. Weather Rev., 97, 163–172, https://doi.org/10.1175/1520-0493(1969)097%3C0163:ATFTEP%3E2.3.CO;2, 1969.

Brooks, H. E., ~~G. W.~~ Carbin, G. W., and ~~P. T.~~ Marsh, ~~2014:~~P. T.: Increased variability of tornado occurrence in the United States~~.~~, Science, 346, 349–352, https://doi.org/10.1126/science.1257460, 2014.

Charney, J. G~~.~~., and ~~J. G.~~ DeVore, ~~1979:~~J. G.: Multiple flow equilibria in the atmosphere and blocking~~.~~, J. Atmospheric Sci., 36, 1205–1216, https://doi.org/10.1175/1520-0469(1979)036%3C1205:MFEITA%3E2.0.CO;2, 1979.

Chen, W. Y. and Van den Dool, H. M.: Atmospheric predictability of seasonal, annual, and decadal climate means and the role of the ENSO cycle: A model study, J. Clim., 10, 1236–1254, https://doi.org/10.1175/1520-0442(1997)010%3C1236:APOSAA%3E2.0.CO;2, 1997.

Childs, S., ~~R. S.~~ Schumacher, R. S., and ~~J. T.~~ Allen, ~~2018:~~J. T.: Cold-season tornadoes: Climatological and meteorological insights~~.~~, Weather Forecast., 33, 671–691, https://doi.org/10.1175/WAF-D-17-0120.1, 2018.

Chu, J.-E., ~~A.~~ Timmermann, A., and ~~J.-Y.~~ Lee, ~~2019:~~J.-Y.: North American April tornado occurrences linked to global sea surface temperature anomalies~~.~~, Sci. Adv., 5, https://doi.org/10.1126/sciadv.aaw9950, 2019.

Cohen, J., Screen, J. A., Furtado, J. C., Barlow, M., Whittleston, D., Coumou, D., Francis, J., Dethloff, K., Entekhabi, D., Overland, J., and Jones, J.: Recent Arctic amplification and extreme mid-latitude weather, Nat. Geosci., 7, 627–637, https://doi.org/10.1038/ngeo2234, 2014.

Cook, A. R~~.~~., and ~~J. T.~~ Schaefer, ~~2008:~~J. T.: The relation of El Nino-Southern Oscillation (ENSO) to winter tornado outbreaks~~.~~, Mon. Weather Rev., 136, 3121–3137, https://doi.org/10.1175/2007MWR2171.1, 2008.

~~———, L.~~Cook, A. R., Leslie, ~~D.~~L., Parsons, D., and ~~J.~~ Schaefer, ~~2017:~~J.: The impact of El Nino-Southern Oscillation (ENSO) on Winter and early Spring U.S. tornado outbreaks~~.~~, J. Appl. Meteorol. Climatol., 56, 2455–2478, https://doi.org/10.1175/JAMC-D-16-0249.1, 2017.

Copernicus Climate Change Service, C. D. S~~., 2018:~~.: Seasonal forecast subdaily data on pressure levels~~.~~ ~~Copernicus Climate Change Service (C3S) Climate Data Store (CDS), accessed 1 June 2025~~, https://doi.org/10.24381/cds.50ed0a73, 2018.

Cwik, P., ~~R. A.~~ McPherson, ~~M. B.~~R. A., Richman, M. B., and ~~A. E.~~ Mercer, ~~2022:~~A. E.: Climatology of 500-hPa geopotential height anomalies associated with May tornado outbreaks in the United States~~.~~, Int. J. Climatol., 43, 893–913, https://doi.org/10.1002/joc.7841, 2022.

Czaja, A~~.~~., and ~~C.~~ Frankignoul, ~~2002:~~C.: Observed Impact of Atlantic SST Anomalies on the North Atlantic Oscillation~~.~~, J. Clim., 15, 606–623, https://doi.org/10.1175/1520-0442(2002)015%3C0606:OIOASA%3E2.0.CO;2, 2002.

~~Duan, W~~Diffenbaugh, N. S., Scherer, M., and ~~C.~~Trapp, R. J.: Robust increases in severe thunderstorm environments in response to greenhouse forcing, Proc. Natl. Acad. Sci. U. S. A., 110, 16361–16366, https://doi.org/10.1073/pnas.1307758110, 2013.

Duan, W. and Wei, ~~2012:~~C.: The ~~"~~"spring predictability ~~barrier'~~barrier" for ENSO predictions and its possible mechanism: Results from a fully coupled model~~.~~, Int. J. Climatol., 33, 1280–1292, https://doi.org/10.1002/joc.3513, 2012.

Elsner, J. B., ~~T. H.~~ Jagger, T. H., and ~~T.~~ Fricker, ~~2016:~~T.: Statistical models for tornado climatology: Long and short-term views~~.~~, PLoS ONE, 11, https://doi.org/10.1371/journal.pone.0166895, 2016.

Gensini, V. A~~.~~., and ~~M. K.~~ Tippett, ~~2019:~~M. K.: Global Ensemble Forecast System (GEFS) predictions of days 1-15 U.S. tornado and hail frequencies~~.~~, Geophys. Res. Lett., 46, 2922–2930, https://doi.org/10.1029/2018GL081724, 2019.

~~———, B. S.~~ Gensini, V. A., Barrett, ~~J. T.~~B. S., Allen, ~~D.~~J. T., Gold, D., and ~~P.~~ Sirvatka, ~~2020:~~P.: The Extended-Range Tornado Activity Forecast (ERTAF) Project~~.~~, Bull. Am. Meteorol. Soc., 101, E700–E709, https://doi.org/10.1175/BAMS-D-19-0188.1, 2020.

Graber, M., ~~R. J.~~ Trapp, R. J., and ~~Z.~~ Wang, ~~2024:~~Z.: The regionality and seasonality of tornado trends in the United States~~.~~, Npj Clim. Atmospheric Sci., 7, https://doi.org/10.1038/s41612-024-00698-y, 2024.

~~———, Z.~~Graber, M., Wang, Z., and ~~R. J.~~ Trapp, ~~2025:~~R. J.: Linking weather regimes to the variability of warm-season tornado activity over the United States~~.~~, Weather Clim. Dyn., 6, 807–816, https://doi.org/10.5194/wcd-6-807-2025, 2025.

Hannachi, A., ~~D. M.~~ Straus, ~~C. L. E.~~D. M., Franzke, ~~S.~~C. L. E., Corti, S., and ~~T.~~ Woollings, ~~2017:~~T.: Low-frequency nonlinearity and regime behavior in the northern hemisphere extratropical atmosphere~~.~~, Rev. Geophys., 55, 199–234, https://doi.org/10.1002/2015RG000509, 2017.

Hersbach, H., ~~and Coauthors, 2020:~~Bell, B., Berrisford, P., Hirahara, S., Horányi, A., Muñoz-Sabater, J., Nicolas, J., Peubey, C., Radu, R., Schepers, D., Simmons, A., Soci, C., Abdalla, S., Abellan, X., Balsamo, G., Bechtold, P., Biavati, G., Bidlot, J., Bonavita, M., De Chiara, G., Dahlgren, P., Dee, D., Diamantakis, M., Dragani, R., Flemming, J., Forbes, R., Fuentes, M., Geer, A., Haimberger, L., Healy, S., Hogan, R. J., Hólm, E., Janisková, M., Keeley, S., Laloyaux, P., Lopez, P., Lupu, C., Radnoti, G., de Rosnay, P., Rozum, I., Vamborg, F., Villaume, S., and Thépaut, J.-N.: The ERA5 global reanalysis~~.~~, Q. J. R. Meteorol. Soc., 146, 1999–2049, https://doi.org/10.1002/qj.3803, 2020.

~~———, and Coauthors, 2023a:~~Hersbach, H., Bell, B., Berrisford, P., Biavait, G., Horányi, A., Munoz Sabater, J., Nicolas, J., Peubey, C., Radu, R., Rozum, I., Schepers, D., Simmons, A., Soci, C., Dee, D., and Thepaut, J.-N.: ERA5 hourly data on pressure levels from 1940 to present~~. Copernicus Climate Change Service~~

~~(C3S) Climate Data Store (CDS), accessed 1 October 2025~~, https://doi.org/10.24381/cds.bd0915c6, 2023a.

~~— —, and Coauthors, 2023b:~~Hersbach, H., Bell, B., Berrisford, P., Biavati, G., Horányi, A., Munoz Sabater, J., Nicolas, J., Peubey, C., Radu, R., Rozum, I., Schepers, D., Simmons, A., Soci, C., Dee, D., and Thepaut, J.-N.: ERA5 hourly data on single levels from 1940 to present~~. Copernicus Climate Change Service (C3S) Climate Data Store (CDS), accessed 1 October 2025~~, https://doi.org/10.24381/cds.adbb2d47, 2023b.

~~Huang, B., and Coauthors, 2017:~~Huang, B., Thorne, P. W., Banzon, V. F., Boyer, T., Chepurin, G., Lawrimore, J. H., Menne, M. J., Smith, T. H., Vose, R. S., and Zhang, H.-M.: Extended Reconstructed Sea Surface Temperature, version 5 (ERSSTv5): Upgrades, validations, and intercomparisons~~.~~, 15 Oct 2017, 30, 8179–8205, https://doi.org/10.1175/JCLI-D-16-0836.1, 2017.

Hurrell, J. W.: Decadal trends in the North Atlantic Oscillation: Regional temperatures and precipitation, Science, 269, 676–679, https://doi.org/10.1126/science.269.5224.676, 1995.

Hurrell, J. W. and Deser, C.: North Atlantic climate variability: The role of the North Atlantic Oscillation, J. Mar. Syst., 79, 231–244, https://doi.org/10.1016/j.jmarsys.2009.11.002, 2010.

Jiang, Q., ~~D. T.~~ Dawson II, ~~L.~~D. T., Funing, L., and ~~D. R.~~ Chavas, ~~2025:~~D. R.: Classifying synoptic patterns driving tornadic storms and associated spatial trends in the United States~~.~~, Npj Clim. Atmospheric Sci., 8, https://doi.org/10.1038/s41612-025-00897-1, 2025.

Knowles, J. B. and Pielke, R. A.: The Southern Oscillation and its effects on tornadic activity in the United States, 15 pp, 2005.

Lau, N.-C.: A diagnostic study of recurrent meteorological anomalies appearing in a 15-year simulation with a GFDL general circulation model, Mon. Weather Rev., 109, 2287–2311, https://doi.org/10.1175/1520-0493(1981)109%3C2287:ADSORM%3E2.0.CO;2, 1981.

Leathers, D. J., Yarnal, B., and Palecki, M. A.: The Pacific/North American teleconnection pattern and United States climate. Part I: Regional temperature and precipitation associations, J. Clim., 4, 517–528, https://doi.org/10.1175/1520-%200442(1991)004,0517:TPATPA.2.0.CO;2., 1991.

Lee, S. H., ~~M. K.~~ Tippett, ~~and L.~~ M. K., and Polvani, ~~2023:~~L. M.: A new year-round weather regime classification for North America~~.~~, J. Clim., 36, 7091–7108, https://doi.org/10.1175/JCLI-D-23-0214.1, 2023.

Lee, S.-K., ~~A. T.~~ Wittenberg, ~~D. B.~~A. T., Enfield, ~~S. J.~~D. B., Weaver, ~~C.~~S. J., Wang, C., and ~~R.~~ Atlas, ~~2016:~~R.: US regional tornado outbreaks and their links to spring ENSO phases and North Atlantic SST variability~~.~~, Environ. Res. Lett., 11, https://doi.org/10.1088/1748-9326/11/4/044008, 2016.

Lepore, C., ~~M. K.~~ Tippett, M. K., and ~~J. T.~~ Allen, ~~2017:~~J. T.: ENSO-based probabilistic forecasts of March-May U.S. tornado and hail activity~~.~~, Geophys. Res. Lett., 44, 9093–9101, https://doi.org/10.1002/2017GL074781, 2017.

Li, X., Hu, Z.-Z., Liang, P., and Zhu, J.: Contrastive influence of ENSO and PNA on variability and predictability of North American winter precipitation, J. Clim., 32, 6271–6284, https://doi.org/10.1175/JCLI-D-19-0033.1, 2019.

Mercer, A. E., ~~C. M.~~ Shafer, C. ~~A.~~M., Doswell III, ~~L. M.~~C. A., Leslie, L. M., and ~~M. B.~~ Richman, ~~2012:~~M. B.: Synoptic composites of tornadic and nontornadic outbreaks~~.~~, Mon. Weather Rev., 140, 2590–2608, https://doi.org/10.1175/MWR-D-12-00029.1, 2012.

Michelangeli, P.-A., ~~R.~~ Vautard, R., and ~~B.~~ Legras, ~~1995:~~B.: Weather regimes: Recurrence and quasi stationarity~~.~~, J. Atmospheric Sci., 52, 1237–1256, https://doi.org/10.1175/1520-0469(1995)052%3C1237:WRRAQS%3E2.0.CO;2, 1995.

Miller, D., ~~Z.~~ Wang, ~~R. J.~~Z., Trapp, R. J., and ~~D. S.~~ Harnos, ~~2020:~~D. S.: Hybrid prediction of weekly tornado activity out to week 3: Utilizing weather regimes~~.~~, Geophys. Res. Lett., 47, https://doi.org/10.1029/2020GL087253, 2020.

Molina, M. J., ~~R. P.~~ Timmer, R. P., and ~~J. T.~~ Allen, ~~2016:~~J. T.: Importance of the Gulf of Mexico as a climate driver for U.S. severe thunderstorm activity~~.~~, Geophys. Res. Lett., 43, 12295–12304, https://doi.org/10.1002/2016GL071603, 2016.

Moore, T. W~~., 2018:~~.: Annual and seasonal tornado trends in the Contiguous United States and its regions~~.~~, Int. J. Climatol., 38, 1582–1594, https://doi.org/10.1002/joc.5285, 2018.

~~——, 2019:~~Moore, T. W.: Seasonal frequency and spatial distribution of tornadoes in the United States and their relationship to the El Nino/Southern Oscillation~~.~~, Ann. Am. Assoc. Geogr., 109, 1033–1051, https://doi.org/10.1080/24694452.2018.1511412, 2019.

Munoz, E~~.~~., and ~~D.~~ Enfield, ~~2011:~~D.: The boreal spring variability of the Intra-Americas low-level jet and its relation with precipitation and tornadoes in the eastern United States~~.~~, Clim. Dyn., 36, 247–259, https://doi.org/10.1007/s00382-009-0688-3, 2011.

National Weather Service~~, 2025~~: 80-year list of severe weather fatalities, available at: https://www.weather.gov/media/hazstat/80year_2024.pdf, 2025.

NCEI~~, 2024~~: U.S. billion-dollar weather and climate disasters, DOI: 10.25921/stkw-w73, 2024.

Niloufar, N., ~~N.~~ Devineni, ~~V.~~N., Were, V., and ~~R.~~ Khanbilvardi, ~~2021:~~R.: Explaining the trends and variability in the United States tornado records using climate teleconnections and shifts in observational practices~~.~~, Sci. Rep., 11, https://doi.org/10.1038/s41598-021-81143-5, 2021.

Ning, L. and Bradley, R. S.: NAO and PNA influences on winter temperature and precipitation over the eastern United States in CMIP5 GCMs, Clim. Dyn., 46, 1257–1276, https://doi.org/10.1007/s00382-015-2643-9, 2015.

NOAA Climate Prediction Center~~,~~: Daily climate mode indices, NOAA/NCEP/CPC [dataset], available at: https://ftp.cpc.ncep.noaa.gov/cwlinks/, 2024a.

NOAA Climate Prediction Center: Oceanic Niño Index (ONI) v5 - Monthly SST anomalies in the Nino 3.4 region, ~~accessed 1 September 2025,~~NOAA/NCEP/CPC [dataset], available at: https://www.cpc.ncep.noaa.gov/products/analysis_monitoring/ensostuff/ONI_v5.php, 2024b.

~~——, 2024b: Daily climate mode indices, accessed 1 September 2025, https://ftp.cpc.ncep.noaa.gov/cwlinks/.~~

Phillips, A. S., Deser, C., and Fasullo, J.: Evaluating modes of variability in climate models, Eos Trans. Am. Geophys. Union, 95, 453–471, https://doi.org/10.1002/2014EO490002, 2014.

Schaefer, J. T.: The critical success index as an indicator of warning skill, Weather Forecast., 5, 570–575, https://doi.org/10.1175/1520-0434(1990)005%3C0570:TCSIAA%3E2.0.CO;2, 1990.

Schneider, R. S., ~~J. T.~~ Schaefer, J. T., and ~~H. E.~~ Brooks, ~~2004:~~H. E.: Tornado outbreak days: An updated and expanded climatology (1875-2003~~). Vol. P5.1 of,~~), 22nd Conference on Severe Local Storms, ~~Hyannis, MA, American Meteorological Society~~2004.

Sherburn, K. D., ~~M. D.~~ Parker, ~~J. R.~~M. D., King, J. R., and ~~G.~~ Lackmann, ~~2016:~~G.: Composite environments of severe and nonsevere high-shear, low-CAPE convective events~~.~~, Weather Forecast., 31, 1899–1927, https://doi.org/10.1175/WAF-D-16-0086.1, 2016.

Soulard, N., Lin, H., and Yu, B.: The changing relationship between ENSO and its extratropical response patterns, Sci. Rep., 9, https://doi.org/10.1038/s41598-019-42922-3, 2019.

Strader, S. M., ~~V. A.~~ Gensini, ~~W. S.~~V. A., Ashley, W. S., and ~~A. N.~~ Wagner, ~~2024:~~A. N.: Changes in tornado risk and societal vulnerability leading to greater tornado impact potential~~.~~, Npj Nat. Hazards, 1, https://doi.org/10.1038/s44304-024-00019-6, 2024.

Thompson, D. W. J. and Wallace, J. M.: Annular Modes in the Extratropical Circulation. Part 1: Month-to-month Variability, J. Clim., 13, 1000–1016, https://doi.org/10.1175/1520-0442(2000)013%3C1000:AMITEC%3E2.0.CO;2, 2000.

Thompson, R. L., Edwards, R., and Hart, J. A.: Close proximity soundings within supercell environments obtained from the rapid update cycle, Weather Forecast., 18, 1243–1261, https://doi.org/10.1175/1520-0434(2003)018%3C1243:CPSWSE%3E2.0.CO;2, 2003.

Tippett, M. K., ~~C.~~ Lepore, C., and ~~M. L.~~ L'Heureux, ~~2022:~~M. L.: Predictability of a tornado environment index from El Nino Southern Oscillation (ENSO) and the Arctic Oscillation~~.~~, Weather Clim. Dyn., 3, 1063–1075, https://doi.org/10.5194/wcd-3-1063-2022, 2022.

~~——,~~Tippett, M. K~~.~~., Malloy, K., and ~~S. H.~~ Lee, ~~2024:~~S. H.: Modulation of U.S. tornado activity by year-round North American weather regimes~~.~~, Mon. Weather Rev., 152, 2189–2202, https://doi.org/10.1175/MWR-D-24-0016.1, 2024.

Trapp, R. J~~., 2013:~~.: Mesoscale-convective processes in the atmosphere~~.~~, Cambridge University Press, 377 pages, https://doi.org/10.1017/CBO9781139047241, 2013.

~~——, 2014:~~Trapp, R. J.: On the significance of multiple consecutive days of tornado activity~~.~~, Mon. Weather Rev., 142, 1452–1459, https://doi.org/10.1175/MWR-D-13-00347.1, 2014.

Vitart, F., Ardilouze, C., Bonet, A., Brookshaw, A., Chen, M., Codorean, C., Deque, M., Ferranti, L., Fucile, E., Fuentes, M., Hendon, H., Hodgson, J., Kang, H.-S., Kumar, A., Lin, H., Liu, G., Liu, X., Malguzzi, P., Mallas, I., Manoussakis, M., Mastrangelo, D., MacLachlan, C., McLean, P., Minami, A., Mladek, R., Nakazawa, T., Najm, S., Nie, Y., Rixen, M., Robertson, A. W., Ruti, P., Sun, C., Takaya, Y., Tolstykh, M., Venuti, F., Waliser, D., Woolnough, S., Wu, T., Won, D.-J., Xiao, H., Zaripov, R., and ~~Coauthors,~~

~~2017:~~Zhang, L.: The subseasonal to seasonal (S2S) prediction project database~~.~~, Bull. Am. Meteorol. Soc., 98, 163–173, https://doi.org/10.1175/BAMS-D-16-0017.1, 2017.

Wallace, J. M. and Gutzler, D. S.: Teleconnections in the geopotential height field during the Northern Hemisphere winter, Mon. Weather Rev., 109, 784–812, https://doi.org/10.1175/1520-0493(1981)109%3C0784:TITGHF%3E2.0.CO;2, 1981.

Wyburn-Powell, C. and Jahn, A.: Large-scale climate modes drive low-frequency regional Arctic sea ice variability, J. Clim., 37, 4313–4333, https://doi.org/10.1175/JCLI-D-23-0326.1, 2024.

Zhang, W., ~~S.~~ S-Y Wang, ~~Y.~~S., Chikamoto, ~~R.~~Y., Gillies, ~~M.~~R., LaPlante, M., and ~~V.~~ Hari, ~~2024:~~V.: A weather pattern responsible for increasing wildfires in the western United States~~.~~, Environ. Res. Lett., 20, https://doi.org/10.1088/1748-9326/ad928f, 2024.

Zhao, J., ~~L.~~ Bai, ~~B.~~L., Zhou, B., and ~~L.~~ Zhang, ~~2025:~~L.: Contributions of Interdecadal Pacific Oscillation, Atlantic Multidecadal Oscillation, and global ocean warming to the secular change in United States tornado occurrence~~.~~, Atmospheric Res., 331, https://doi.org/10.1016/j.atmosres.2025.108689, 2025.

Formatted: Font: +Body (Calibri)
Formatted: Font: +Body (Calibri)
Formatted: Font: +Body (Calibri), Not Italic
Formatted: Font: +Body (Calibri)
Formatted: Font: +Body (Calibri), Not Bold
Formatted: Font: +Body (Calibri)
Formatted: Font: +Body (Calibri)

Formatted: Font: +Body (Calibri)
Formatted: Font: +Body (Calibri)
Formatted: Font: +Body (Calibri)
Formatted: Font: +Body (Calibri)
Formatted: Font: +Body (Calibri)
Formatted: Font: +Body (Calibri)
Formatted: Font: +Body (Calibri)
Formatted: Font: +Body (Calibri)
Formatted: Font: +Body (Calibri)
Formatted: Font: +Body (Calibri), Not Italic
Formatted: Font: +Body (Calibri)
Formatted: Font: +Body (Calibri), Not Bold
Formatted: Font: +Body (Calibri)
Formatted: Font: +Body (Calibri)
Formatted: Font: +Body (Calibri)
Formatted: Font: +Body (Calibri)
Formatted: Font: +Body (Calibri)
Formatted: Font: +Body (Calibri)
Formatted: Font: +Body (Calibri)
Formatted: Font: +Body (Calibri)
Formatted: Font: +Body (Calibri), Not Italic
Formatted: Font: +Body (Calibri)
Formatted: Font: +Body (Calibri), Not Bold
Formatted: Font: +Body (Calibri)
Formatted: Font: +Body (Calibri)